Supplementary figure legends

Figure S1. Antibody specificity test using ELISA. The specificity of three H3K9me3 antibodies against various methylated or un-methylated histone peptides was tested using an ELISA assay. The plates were coated with 1μg/ml peptides overnight. Then the plates were blocked with 3% BSA in PBS at room temperature for 30 minutes and incubated with the primary antibodies (1:3000) for 3 hours at room temperature. The primary H3K9me3 antibodies tested are 39161 (Active Motif), 07-442 (Millipore), and 8898 (Abcam). The primary antibodies were diluted in ChIP reaction buffer (Millipore ChIP Kit, 90% Sample dilution buffer with 10% Lysis buffer). After rinses with PBS, plates were incubated with HRP-conjunct secondary antibodies (Promega) diluted in PBS for 1 hour at room temperature. After then rinses with PBS, the plates were incubated with the substrate and stop solution (R&D) and lastly read the absorbance at A450 (ELISA signal) and A540 (correction for plate background). The Y-axis represents the relative activity value determined using A450-A540.

Figure S2. Comparison of H3K9me3 signal around SETDB1 peaks based on different H3K9me3 ChIP-seq experiments. (**A-H**) Density plot showing the enrichment of H3K9me3 within the ±1 kb regions of the SETDB1 binding sties (from Yuan *et al.*) based on eight different ChIP-seq experiments. Respective H3K9me3 ChIP-seq data for mouse ES cells generated in current research, and previous researches from Yuan *et al.* (GSE17642), Bilodeau *et al.* (GSE18371), Karimi *et al.* (two ES cell lines: J1 and TT2, GSE29413) were utilized. Kernel density estimation, a non-parametric way to estimate the probability density function of a random variable, was used here. The scale of y-axis indicates the possibility to observe H3K9me3 ChIP-seq reads intensity (log_{10}-transformed) as a certain value (for example, x) in SETDB1 binding sites. (**I-P**) Average profiles of H3K9me3 ChIP-seq signal around SETDB1 solo and

ensemble peaks. SETDB1 solo and ensemble peaks were defined using SETDB1 ChIP-seq data from Yuan *et al.* and H3K9me3 ChIP-seq data from current research. All profiles were centered at the middle 1 bp of the SETDB1 binding regions. The average signal represents the average value of wiggle files (generated by MACS2) across a category of binding regions per 50-bp interval.

Figure S3. Confirmation of SETDB1 binding at SETDB1 targets by ChIP-qPCR. ChIP-qPCR was applied to confirm the SETDB1 binding at the SETDB1 solo and ensemble peaks. *Setdb1* iKO mES cells were treated with or without Tamoxifen and subjected to ChIP with SETDB1 antibody. Anti-rabbit normal IgG was used as the negative control. The selected SETDB1 peak loci were marked by their nearby gene symbols (*Atf4, Lhx2, Ascl1* for SETDB1 solo peaks; *Fam21, Gm6792, Sfi1* for SETDB1 ensemble peaks). Deletion of *Setdb1* diminished SETDB1 binding at all of these sites.

Figure S4. Examination of H3K9me1 and H3K9me2 levels at SETDB1 solo and ensemble peaks. ChIP-qPCR was applied to assess H3K9me1 and H3K9me2 levels at selected SETDB1 solo and ensemble peaks, respectively. It appears that SETDB1 solo peaks are generally devoid of H3K9me1 and H3K9me2 as well. The selected SETDB1 peak loci were marked by their nearby gene symbols (*Atf4, Lhx2, Ascl1, Foxa1, Tbx3* for SETDB1 solo peaks; *Fam21, Gm6792, Sfi1* for SETDB1 ensemble peaks).

Figure S5. Confirmation of *Setdb1* deletion in iKO mES cells before neural differentiation. The iKO cells were culture in adherent and treated with Tamoxifen for three days to induce *Setdb1* deletion. The deletion efficiency was confirmed by western blot analysis.

Figure S6. Neural differentiation upon Tamoxifen treatment in control D3

mouse ES cells. Control D3 cells were treated and assessed for neural differentiation the same as in iKO cells (**Fig. 2C**). No increased neural differentiation was seen from the Tamoxifen treatment. Scale bar = 50 μm (100 μm in the inserts).

Figure S7. Relative binding level for 43 TFs at all SETDB1 ensemble and neural unrelated solo peak loci. (**A-B**) The calculation of relative binding level was in the same way described for **Fig 3A** and the horizontal line represented the average binding intensity across all SETDB1 peaks.

Figure S8. Summary of GO biological process enrichment analysis for target genes of SETDB1 solo peaks. (A) SETDB1 solo peaks were divided into 3 groups based on the peak calling cutoffs for H3K9me3 data from current research. The looser the cutoff for H3K9me3 peak calling was, the more stringent standard for SETDB1 solo peaks would be. Each group stands for the SETDB1 solo peaks defined with certain stringent standard. **(B)** GO biological process enrichment analysis of target genes for different groups of SETDB1 solo peaks via DAVID interface (http://david.abcc.ncifcrf.gov/). Fisher's exact test and Benjamini correction were performed.

Figure S9. Average profile of H3K27me3, EZH2, SUZ12 and RNF2 round the SETDB1 solo peaks generated by different MACS cutoffs. (**A-D**) Solo peak numbers in different categories were listed in Figure S7 (A). All binding sites were extended to 10,000 bp and aligned by the center of the peak region detected by MACS2.

Figure S10. H3K9me3 and H3K27me3 enrichment profiles among SETDB1 targets. X-axis stands for normalized signal of H3K9me3 and Y-axis represents the normalized signal of H3K27me3 in control ES cells. SETDB1 binding sites were divided into two groups, solo and ensemble peaks and then

extended to the same width (5 kb upstream and downstream of peak center). The red dot points represent SETDB1 ensemble peaks whilst the green ones stand for SETDB1 solo peaks. For most SETDB1 solo peak regions, signal of H3K9me3 is comparative lower than that in SETDB1 ensemble peak region but the H3K27me3 enrichment level is much higher at a subset of SETDB1 solo peaks.

Figure S11. Confirmation of target knocking down efficiency of shEZH2. *Setdb1* iKO mES cells were cultured in adherent and infected with lentiviral shRNA against EZH2. 48 hours after the infection, the cells were selected in 1 μg/ml puromycin for another 48 hours to enrich infected cells. The target knocking down efficiency was assessed by Western blot analysis. The shRNA efficiently knocked down EZH2 expression accompanied by a significant reduction of global H3K27me3 as compared with the control shRNA (scramble sequence) or the no virus infected cells.

Figure S12. H3K27me3 level variation at all ±10-kb regions of EZH2 peak loci before and after *Setdb*1 iKO. Only EZH2 peaks with enriched H3K27me3 signal before Tam treatment were included in this analysis (biological replicate pair 2 of current research). Those EZH2 peaks were divided into two categories based on the overlap status with SETDB1 binding: with SETDB1 binding (475 peaks) and without SETDB1 binding (14,143 peaks). Two-sided Welch's *t* test was performed for the change of H3K27me3 between the two groups (** $P < 0.01$).

Figure S13. *Setdb1* deletion does not affect overall protein complex stability. *Setdb1* iKO mES cells were treated with Tamoxifen for three days and assayed for EZH2, SUZ12 expression and histone H3K27 methylation by Western blot analysis. No reduction of EZH2, SUZ12 protein or global H3K27 methylation was seen.

Figure S14. Quality control of H3K9me3 and H3K27me3 ChIP-seq data in this study. (**A-H**) Correlation between H3K9me3 or H3K27me3 ChIP-seq signals and gene expression level was evaluated. One public RNA-seq dataset in mES (GSM1499144) was used and all genes were divided into three categories according to their FPKM values: low (0~10), moderate (10~100), and high (>100). For each H3K9me3 (A-D) or H3K27me3 (E-H) ChIP-seq biological replicate generated in this study, the average signal profiles across gene bodies for each gene category were drawn. (I-J) Fold enrichment score was used to demonstrate the signal enrichment for the MACS2-detected peaks in each H3K9me3 (I) or H3K27me3 (J) ChIP-seq experiment.

Figure S15. Correlation between ChIP-seq datasets generated in this study and public H3K9me3 or H3K27me3 ChIP-seq datasets in mES. (**A**) H3K9me3 ChIP-seq data for mES cells generated in current research, and previous researches from Yuan *et al.* (GSE17642), Bilodeau *et al.* (GSE18371), Karimi *et al.* (two ES cell lines: J1 and TT2, GSE29413) were used. Pearson correlation coefficient between signals at promoter regions (from 2kb upstream to 2kb downstream of TSS) of any two H3K9me3 ChIP-seq datasets was calculated. (B) H3K27me3 ChIP-seq data for mES cells generated in current research (without Tam treatment), and previous researches from Lienert *et al.* (GSE27827) and Stadler *et al.* (GSE30203) were utilized. Pearson correlation coefficient between signals at promoter regions (from 2kb upstream to 2kb downstream of TSS) of any two H3K27me3 ChIP-seq datasets was calculated.

Supplementary tables

Table S1. List of transcription regulators used in the measurement for the level

of co-binding between SETDB1 and other factors

Transcription regulator	Peak number	GEO Accession ID
ATF7IP	5064	GSE26680
CHD7	5352	GSE22341
MYC	6184	GSE11431
CTCF	30300	GSE25777
CTR9	2182	GSE20530
DPY30	36708	GSE26136
E2F1	29936	GSE11431
ESRRB	83541	GSE11431
EZH2	18301	GSE18776
JARID2	7292	GSE18776
KDM2A	28556	GSE18588
KDM5A	9291	GSE18776
KLF4	11987	GSE11431
LAMINB	52567	GSE28247
MED1	26148	GSE22557
MED12	28541	GSE22557
MTF2	6255	GSE16526
NANOG	19318	GSE11724
NIPBL	14357	GSE22557
MYCN	7742	GSE11431
NR5A2	3072	GSE19019
POU5F1	26804	GSE11724
EP300	3290	GSE22341
REST	9224	GSE27841
RBBP5	12656	GSE22934
RNAP2	18491	GSE12680
RNF2	8657	GSE26680
SETDB1	5882	GSE17642
SMAD3	2040	GSE21614
SMARCA4	3780	GSE14344
SMC1A	60633	GSE22557
SMC3	31443	GSE22562
SOX2	4516	GSE11431
STAT3	6355	GSE11431
SUPT5H	8215	GSE20530
SUZ12	38174	GSE18776
TAF1	7992	GSE30959
TAF3	51014	GSE30959
TCF3	6113	GSE11724
TCFCP2L1	43947	GSE11431
TET1	34697	GSE26832
WDR5	4877	GSE22934

WHSC2	21684	GSE20530
ZFX	13784	GSE11431

Forty-three transcription factors known to be involved in ES cell regulation were selected for co-binding analysis with SETDB1. Listed are the factor name, the number of detected peak and the GEO accession ID from which the data were generated.

Table S2. List of primers used in this study

ChIP qPCR primers	Sequences (5'-- 3')
Ascl1	GAACCCGCCATAGAGTTCAA
	GTTGGTCAACCTGGGTTTTG
Lhx2	AGTGGAAGGGGAGTGGAAGT
	GGTCACGATCAACGGAAAGT
Atf4	CGTCAGAGCTTTGGCTAGGT
	GGGGTAACTGTGGCGTTAGA
Sfi1	AGACTCCCAATACCCACACG
	GCCTCCCACAAATGACTGTT
Gm6792	CACTTCCAGGCAGCTAGGAC
	CAGAATTCCCAGGCTGACAT
Fam21	TGGGATACTTGCCTTTCCTG
	TTCTTGGCAATGTGTGTGGT
Faah	AACGGTCAAGGTCAAGCCTA
	TTCTGAGGACCCTGGCTTAG
Pou3f1	GTTCTCGCAGACCACCATCT
	GGCTTGGGACACTTGAGAAA
Tcfap2e	GGACCCGAGTCTACTCACCA
	ACCCCGTACCTTCTGGACTC
Foxo6	GGTGCCAGGACTGGTTAAGA
	TAAGCCACCCAACTCCAATC
Rnf220	AGGACAGCCAGTTAGCCTGA
	CTCCAGCCAGCCTGCTATAC
Tbx3	GCTGCTGCGAACTCTCTTCT
	ACCAATTGTGTGGCTGCATA
Foxa1	GCAACCGGGTCAAGTTGGT
	CAAGTCGTTGGAGTAGTTGGG
Nr2f1	CACCAAGGCGAGAGAGAAAG
	ACAGGAACTGTCCCATCGAC

RT qPCR primers	Sequences (5'--3')
Foxa2	CCCTACGCCAACATGAACTCG

	GTTCTGCCGGTAGAAAGGGA
Pax7	TCTCCAAGATTCTGTGCCGAT
	CGGGGTTCTCTCTCTTATACTCC
Nr2f2	TCAACTGCCACTCGTACCTG
	CCATGATGTTGTTAGGCTGCAT
Nr2f1	GCACTACGGCCAATTCACCT
	TTGGAGGCATTCTTCCTCGC
Hmx2	CCAAGCCCTAAGCACCATACC
	TCCTTAAAGTCCGGGTGAGAAG
Zic1	CAGTATCCCGCGATTGGTGT
	GCGAACTGGGGTTGAGCTT
Lhx5	AATGTGTTCAATGCTGCGAGT
	AAAGCGCCTGAAAAAGTCGTT
Hoxc8	CTTCGTCAACCCCCTGTTTTC
	GTCTTGGACGTGGTGCGAG
Evx1	GAGAGCCGAAAGGACATGGTT
	CTGCCTGCTAGTCCATCGAC
Ascl1	GCAACCGGGTCAAGTTGGT
	CAAGTCGTTGGAGTAGTTGGG
Uncx	ACCCGCACCAACTTTACCG
	TGAACTCGGGACTCGACCA
Hoxd3	ATACTACGAGAACCCAGGACTC
	CAGGTCTCATACAGCTACCATTG
Fezf1	ACGCGACCACCAAAATGCTA
	TCGACGAGTTGAGATGCAGAG
Hoxb8	TGCGCCCCAATTATTATGACTG
	AACTCCTGGATTTGCGAAGGG
Gfra1	CACTCCTGGATTTGCTGATGT
	AGTGTGCGGTACTTGGTGC
Hoxd9	GCACCCTCAGCAACTACTACG
	AAAACTACACGAGGCGAACTC
Fev	ACGCCTACCGCTTTGACTTC
	AAGCTGCCATCAAGTTGAGTT
Hoxb2	ATTCGCCTTTTCTACCGGACC
	GGGCTATCGAGAGAACCCTG
Irx5	TACAGCACCAGCGTCATTTCG
	GAGCCCACGTAAGAGAAGGC
Barhl2	GCGGGTCGAGTTTTGGAATAG
	GCTCCTAAAATCCGTTGTCCTC
Lrp2	GAAAGCTGGACAAGACTGAGTT
	GGCAGTGGTCTGTGAGAATTT
Foxa1	ACATTCAAGCGCAGCTACCC
	TGCTGGTTCTGGCGGTAATAG
Sema6a	CGAGACGGGTATGAGTCTAGG

	CCTGGTGGTTATGAGAGGACAC
Lmx1b	TCCTGGCACGAGGAGTGTT
	AACTCGGTAGGGGCGATCTT
Pax3	TTTCACCTCAGGTAATGGGACT
	GAACGTCCAAGGCTTACTTTGT
Satb2	GCCGTGGGAGGTTTGATGATT
	ACCAAGACGAACTCAGCGTG
Foxg1	CAAGGCTGACGCACTTGGA
	CTTGCCGTTCTTCTTGTCGC
Hoxb3	GCACCTGGAGGGTGACTAC
	CCCCCGTTATTGCTGTTGC
Six1	ATGCTGCCGTCGTTTGGTT
	CCTTGAGCACGCTCTCGTT
Otp	CAGGCTAGGTATGAAAGATGCC
	GAAGCAGGGGTAGAGCCCA
Lhx2	CTGTTCCACAGTCTGTCGGG
	CAGCAGGTAGTAGCGGTCAG
Gfra2	TCTTTTTAGACGAAACCCTCCG
	CCAGCATGGTATTGCGATCC
Egr3	TTGCCTGACAATCTGTACCCC
	TAATGGGCTACCGAGTCGCT
Nkx2-1	AGGACACCATGCGGAACAG
	CCATGCCGCTCATATTCATGC
Neurog2	AACTCCACGTCCCCATACAG
	GAGGCGCATAACGATGCTTCT
Pitx1	GCCTTCAAGGGAGGCATGAG
	GATTCGCTGGCGGAGTTCTC
Sall3	TGGAGGTATCTACGGACAAGG
	GGGTCACATTGGTACTAGGCA
Tbx3	AGATCCGGTTATCCCTGGGAC
	CAGCAGCCCCCACTAACTG
Prdm6	GGAGCCTAGTAAGTCGAGCTG
	GGACGTTCAAGTTTTCATCCTGG
Pou4f2	TGGACATCGTCTCCCAGAGTA
	GTGTTCATGGTGTGGTAAGTGG
Zic2	CAAGGTCCGGGTGCTTACC
	ATTAAAGGGAGGCCCCGAATA
Hnf1b	AGGGAGGTGGTCGATGTCA
	TCTGGACTGTCTGGTTGAACT
Sema5b	GAAGCCGTGGGTCTTTAACTT
	CAAGAGCAAGCTGGGAGAAAT
Otx2	TATCTAAAGCAACCGCCTTACG
	GCCCTAGTAAATGTCGTCCTCTC
Rax	TGGGCTTTACCAAGGAAGACG

Eomes	GGTAGCAGGGCCTAGTAGCTT
	GCGCATGTTTCCTTTCTTGAG
	GGTCGGCCAGAACCACTTC
Six3	GCTCCCGGCTTCTCTTACC
	CGGCGAAGTTTGGCAACAAG
Ascl2	AAGCACACCTTGACTGGTACG
	AAGTGGACGTTTGCACCTTCA
Sim1	ACAGGAGTACGAGATCGAACG
	CTCTGTCACAGCACTCGGAG
Faah	CCCTGCTCCAACTGGTACAG
	TCACAGTCAGTCAGATAGGAGG
Bmp1	ATGGGGTCTCTGGTTCTGC
	CAATACCATCTTGCTCCGTGAA
Pou3f1	TACCGCGAAGTGCAGAAGC
	CGTGGGTAGCCATTGAGGG
Alx1	GAGCCCGCCAAGTAAAAACAG
	GTCGCTTTGCCGTAAAAGGAC
Foxo6	CCCCGGACAAGAGACTCAC
	CGACAGGTTGTGCCGAATG
Fgf2	CCAGGACAGTATAGTGGAGATCC
	AGTAGACCCGCGACCCATAG
Hes5	AGTCCCAAGGAGAAAAACCGA
	GCTGTGTTTCAGGTAGCTGAC
Hoxa1	CCACCAGGGTTATGCTGGG
	CGTGGAGAGGGGATAAGGAGTTA
Cbx2	GGCTGGTCCTCCAAACACAA
	CCCTGGGTCTCTTGCCTCT
Gbx2	CAACTTCGACAAAGCCGAGG
	ACTCGTCTTTCCCTTGCCCT
Setdb1	GGAGGAACTTCGTCAGTACATTG
	TCTTTCTGTAGTACCCACGTCTC
Gapdh	AATGGATTTGGACGCATTGGT
	TTTGCACTGGTACGTGTTGAT

Table S3. Summary of ChIP-seq datasets generated in this study.

ChIP-seq experiment	Uniquely mapped reads	Library complexity
H3K9me3 Replicate 1 (single-end)	22.7 M	0.591
H3K9me3 Replicate 2 (paired-end)	14.3 M	0.810
H3K9me3 Replicate 3 (paired-end)	16.6 M	0.831

H3K9me3 Replicate 4 (paired-end)	15.4 M	0.838
H3K27me3 DMSO-treated Replicate 1 (single-end)	18.6 M	0.935
H3K27me3 Tam-treated Replicate 1 (single-end)	22.8 M	0.655
H3K27me3 DMSO-treated Replicate 2 (paired-end)	24.5 M	0.763
H3K27me3 Tam-treated Replicate 2 (paired-end)	24.7 M	0.587

Figure S1

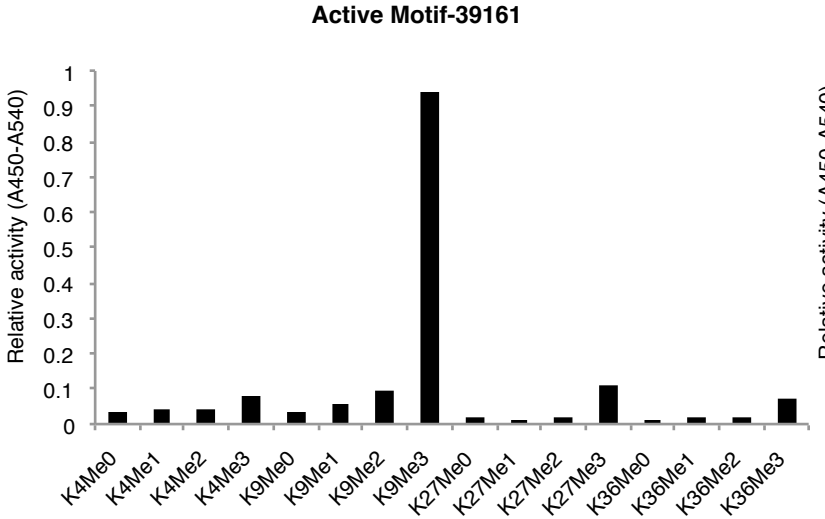
Active Motif-39161
Relative activity (A450-A540)
1
0.9
0.8
0.7
0.6
0.5
0.4
0.3
0.2
0.1
0
K4Me0
K4Me1
K4Me2
K4Me3
K9Me0
K9Me1
K9Me2
K9Me3
K27Me0
K27Me1
K27Me2
K27Me3
K36Me0
K36Me1
K36Me2
K36Me3

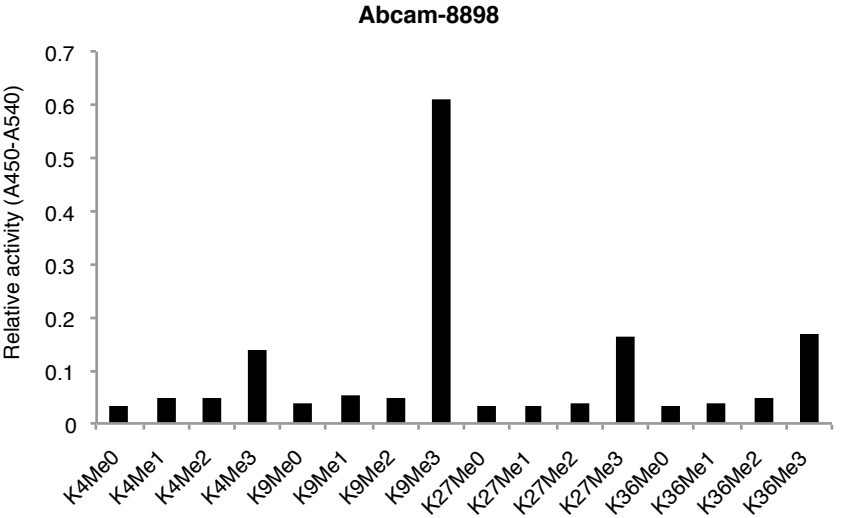
Abcam-8898
Relative activity (A450-A540)
0.7
0.6
0.5
0.4
0.3
0.2
0.1
0
K4Me0
K4Me1
K4Me2
K4Me3
K9Me0
K9Me1
K9Me2
K9Me3
K27Me0
K27Me1
K27Me2
K27Me3
K36Me0
K36Me1
K36Me2
K36Me3

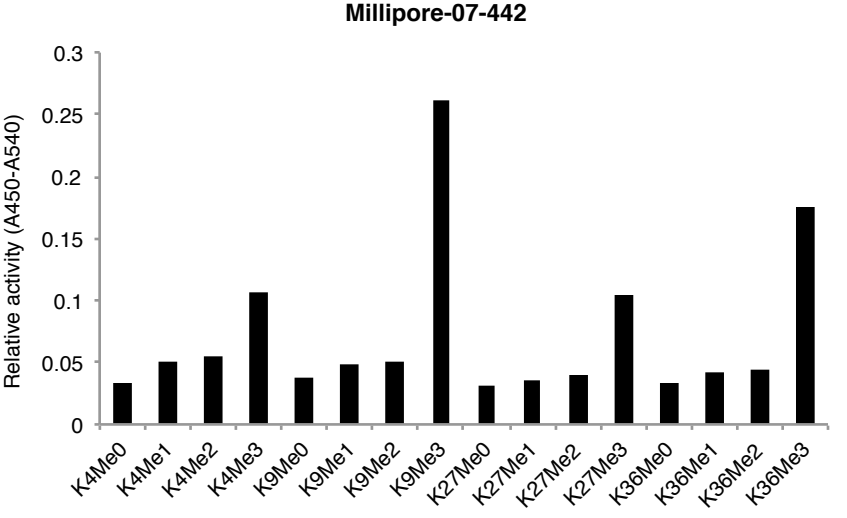
Millipore-07-442
Relative activity (A450-A540)
0.3
0.25
0.2
0.15
0.1
0.05
0
K4Me0
K4Me1
K4Me2
K4Me3
K9Me0
K9Me1
K9Me2
K9Me3
K27Me0
K27Me1
K27Me2
K27Me3
K36Me0
K36Me1
K36Me2
K36Me3

Figure S2

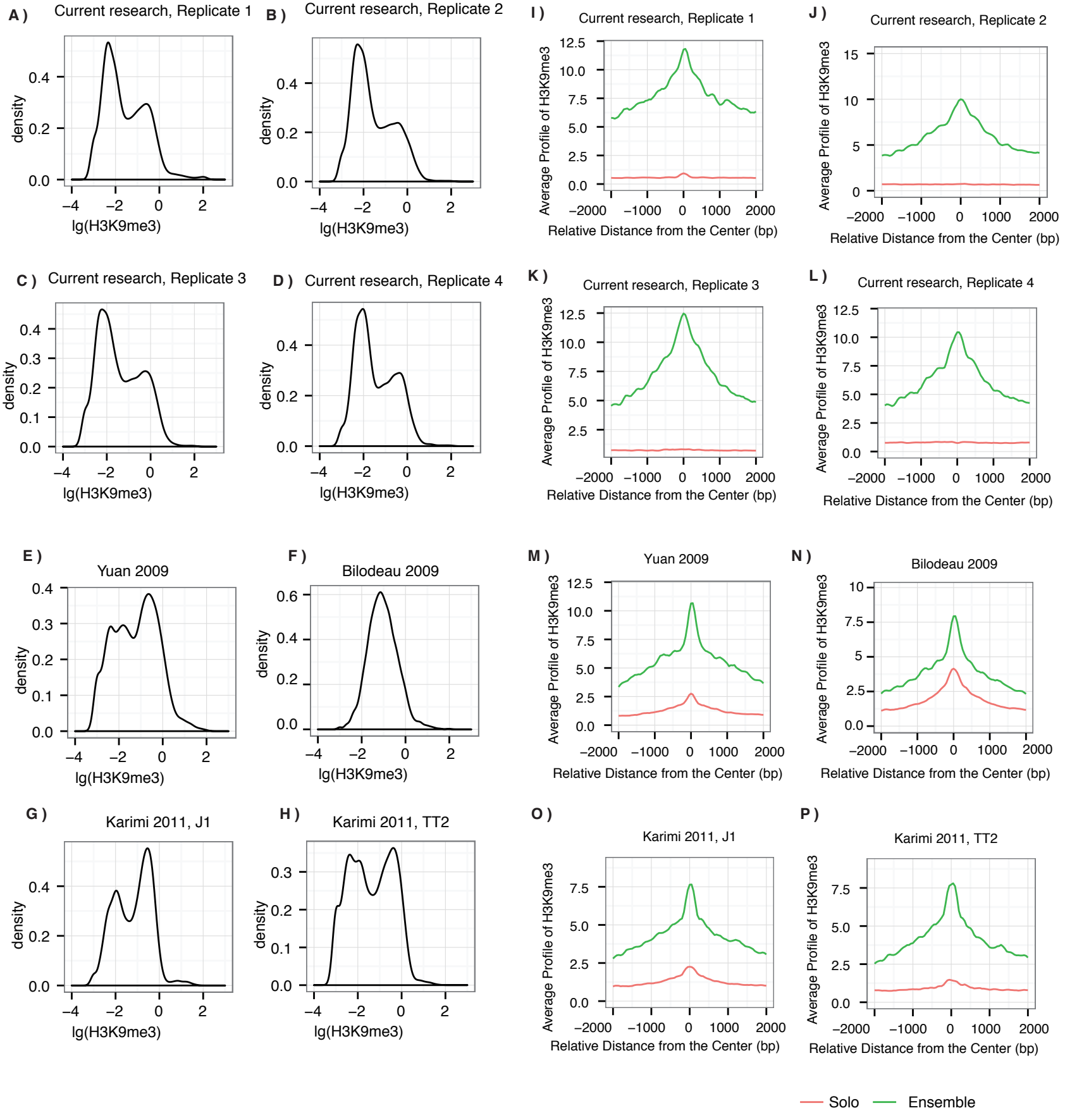
A)
Current research, Replicate 1
B)
Current research, Replicate 2
I)
Current research, Replicate 1
J)
Current research, Replicate 2
C)
Current research, Replicate 3
D)
Current research, Replicate 4
K)
Current research, Replicate 3
L)
Current research, Replicate 4
E)
Yuan 2009
F)
Bilodeau 2009
M)
Yuan 2009
N)
Bilodeau 2009
G)
Karimi 2011, J1
H)
Karimi 2011, TT2
O)
Karimi 2011, J1
P)
Karimi 2011, TT2
density
lg(H3K9me3)
Average Profile of H3K9me3
Relative Distance from the Center (bp)
Solo
Ensemble

Figure S3

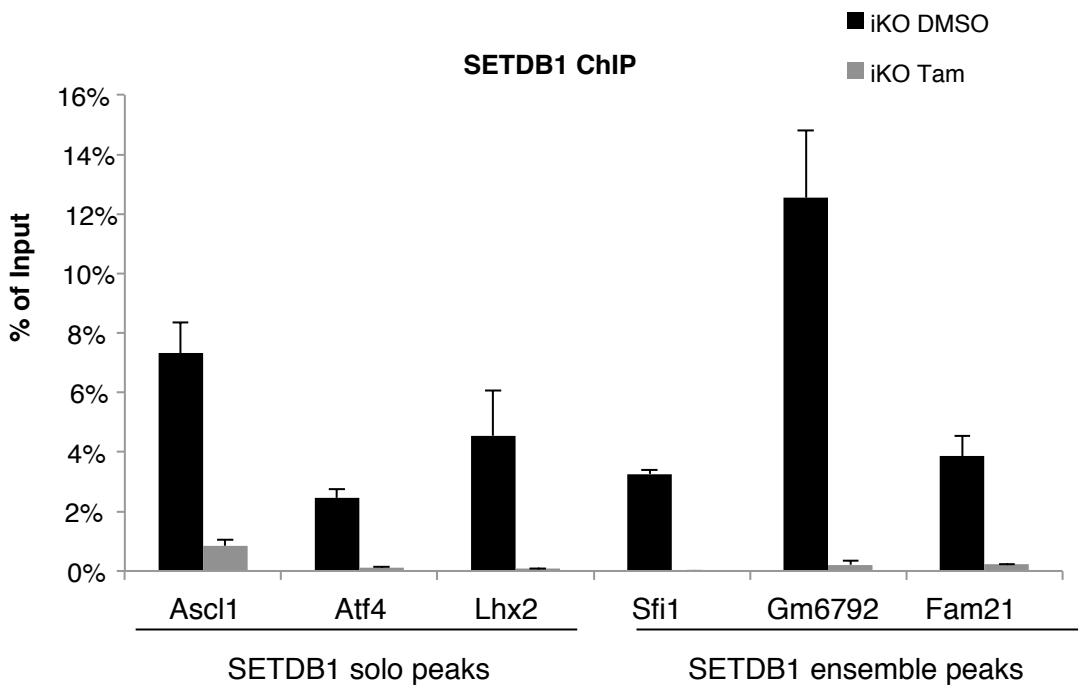
SETDB1 ChIP
iKO DMSO
iKO Tam
% of Input
16%
14%
12%
10%
8%
6%
4%
2%
0%
Ascl1
Atf4
Lhx2
Sfi1
Gm6792
Fam21
SETDB1 solo peaks
SETDB1 ensemble peaks

Figure S4

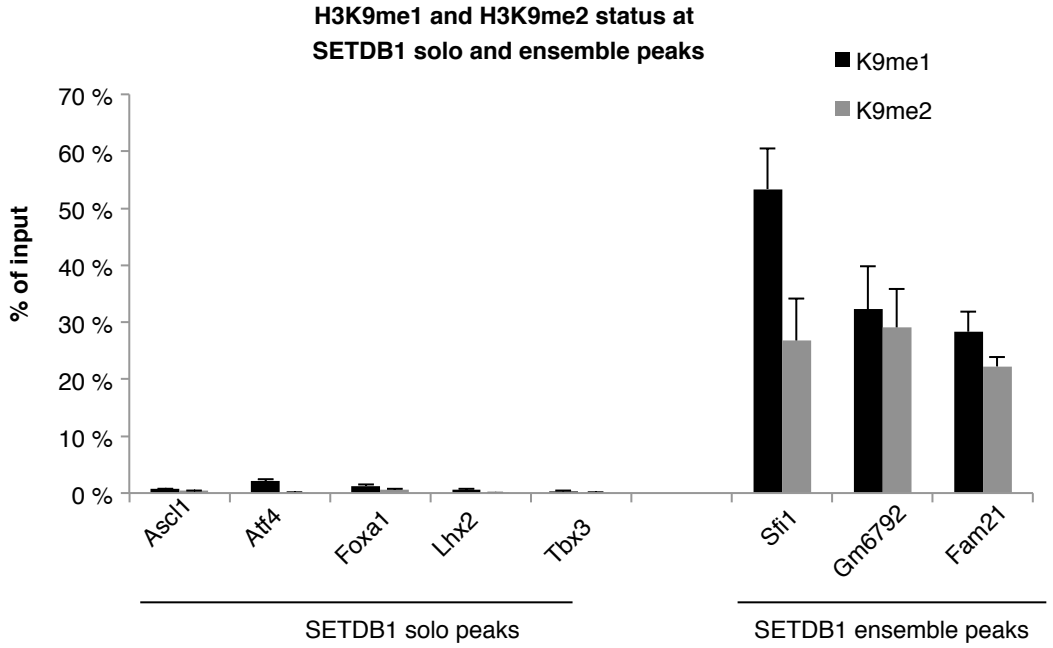
H3K9me1 and H3K9me2 status at
SETDB1 solo and ensemble peaks
K9me1
K9me2
% of input
70 %
60 %
50 %
40 %
30 %
20 %
10 %
0 %
Ascl1
Atf4
Foxa1
Lhx2
Tbx3
Sfi1
Gm6792
Fam21
SETDB1 solo peaks
SETDB1 ensemble peaks

Figure S5

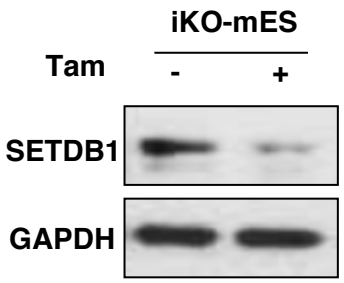

Figure S6

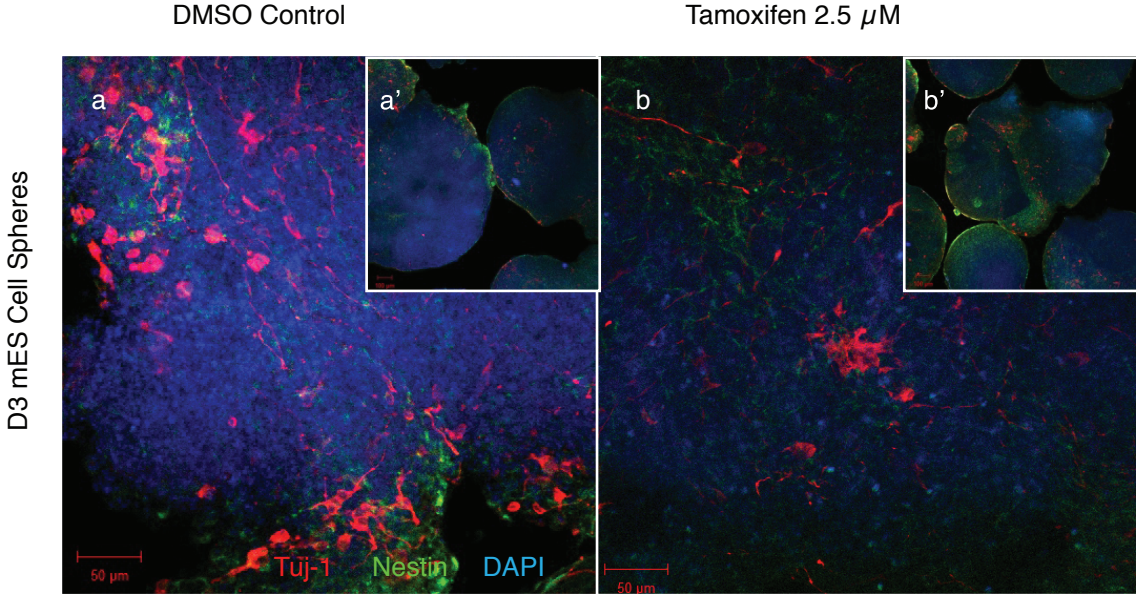
DMSO Control
Tamoxifen 2.5 μM
D3 mES Cell Spheres
a
a'
b
b'
50 μm
Tuj-1
Nestin
DAPI
50 μm

Figure S7

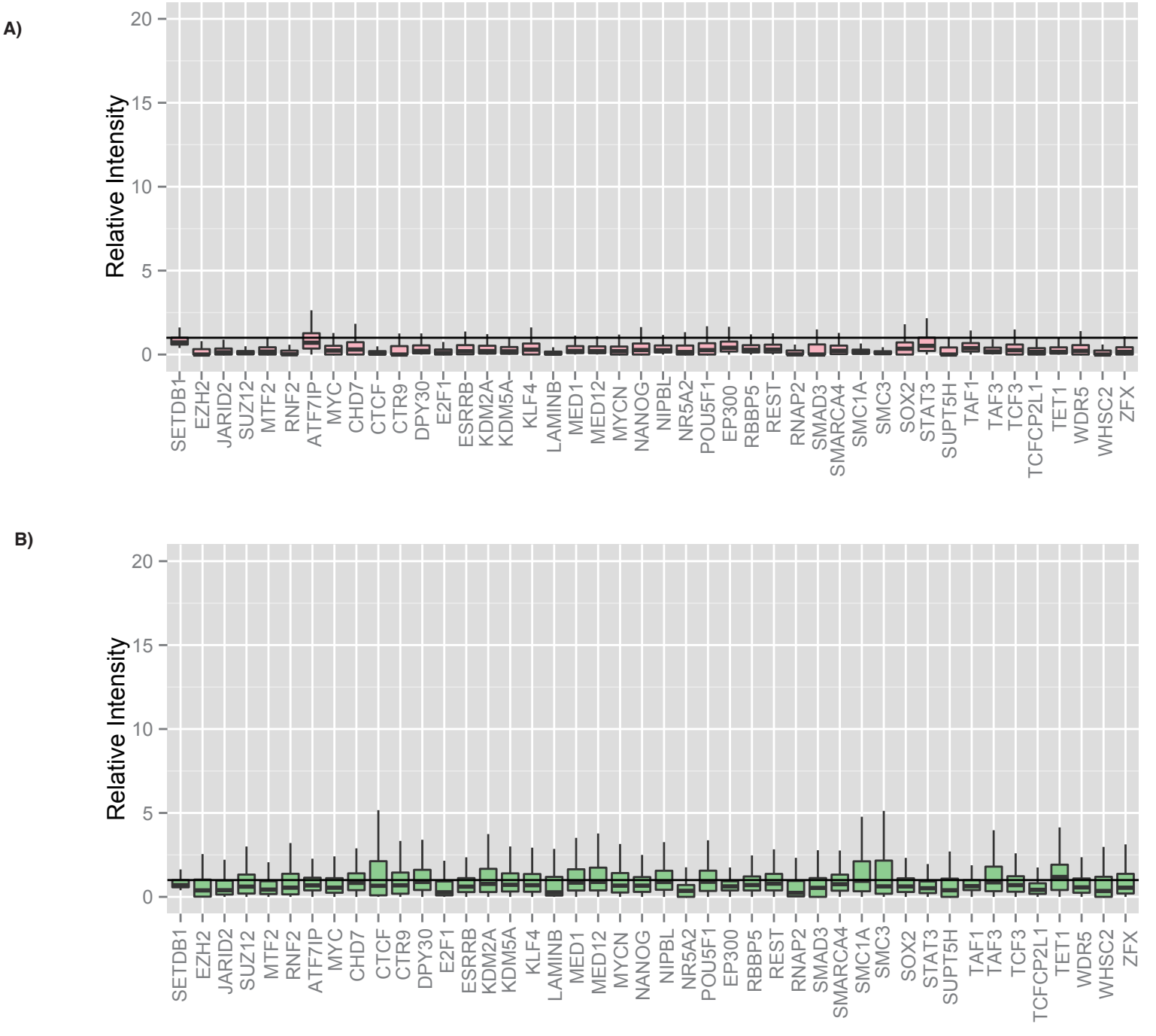
A)
Relative Intensity
20
15
10
5
0
SETDB1
EZH2
JARID2
SUZ12
MTF2
RNF2
ATF7IP
MYC
CHD7
CTCF
CTR9
DPY30
E2F1
ESRRB
KDM2A
KDM5A
KLF4
LAMINB
MED1
MED12
MYCN
NANOG
NIPBL
NR5A2
POU5F1
EP300
RBBP5
REST
RNAP2
SMAD3
SMARCA4
SMC1A
SMC3
SOX2
STAT3
SUPT5H
TAF1
TAF3
TCF3
TCFCP2L1
TET1
WDR5
WHSC2
ZFX
B)
Relative Intensity
20
15
10
5
0
SETDB1
EZH2
JARID2
SUZ12
MTF2
RNF2
ATF7IP
MYC
CHD7
CTCF
CTR9
DPY30
E2F1
ESRRB
KDM2A
KDM5A
KLF4
LAMINB
MED1
MED12
MYCN
NANOG
NIPBL
NR5A2
POU5F1
EP300
RBBP5
REST
RNAP2
SMAD3
SMARCA4
SMC1A
SMC3
SOX2
STAT3
SUPT5H
TAF1
TAF3
TCF3
TCFCP2L1
TET1
WDR5
WHSC2
ZFX

Figure S8

A)

SETDB1 solo peak Group	H3K9me3 MACS2 callpeak Cutoff	Solo Peak number	Gene number (Refseq ID)
Loose	q 0.01 ~ q 0.001	534	189
Moderate	p 0.001 ~ q 0.01	579	185
Stringent	p 0.001	2110	1260

B)

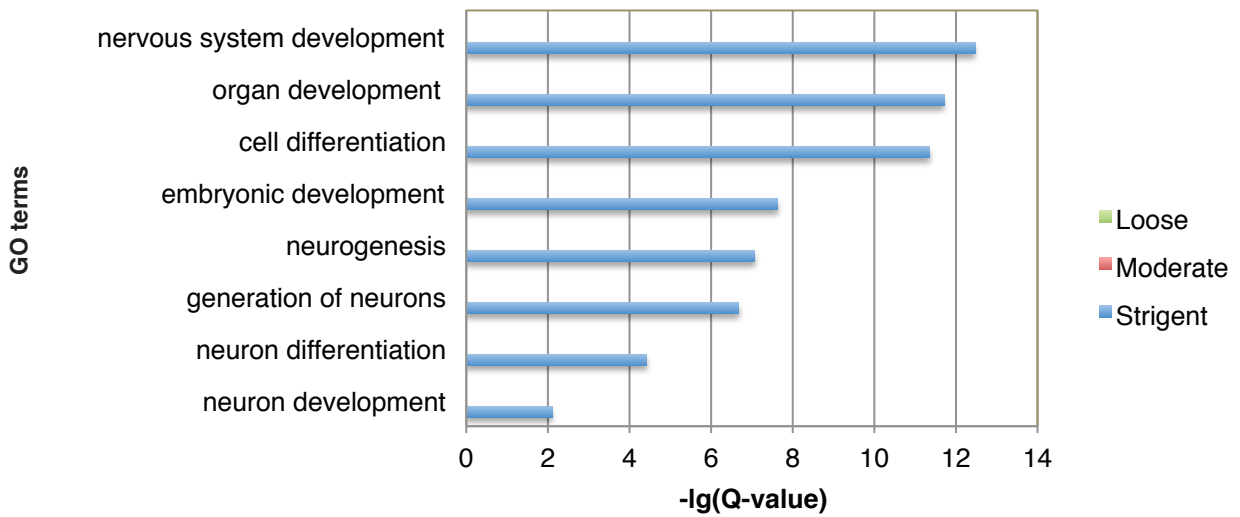

Figure S9

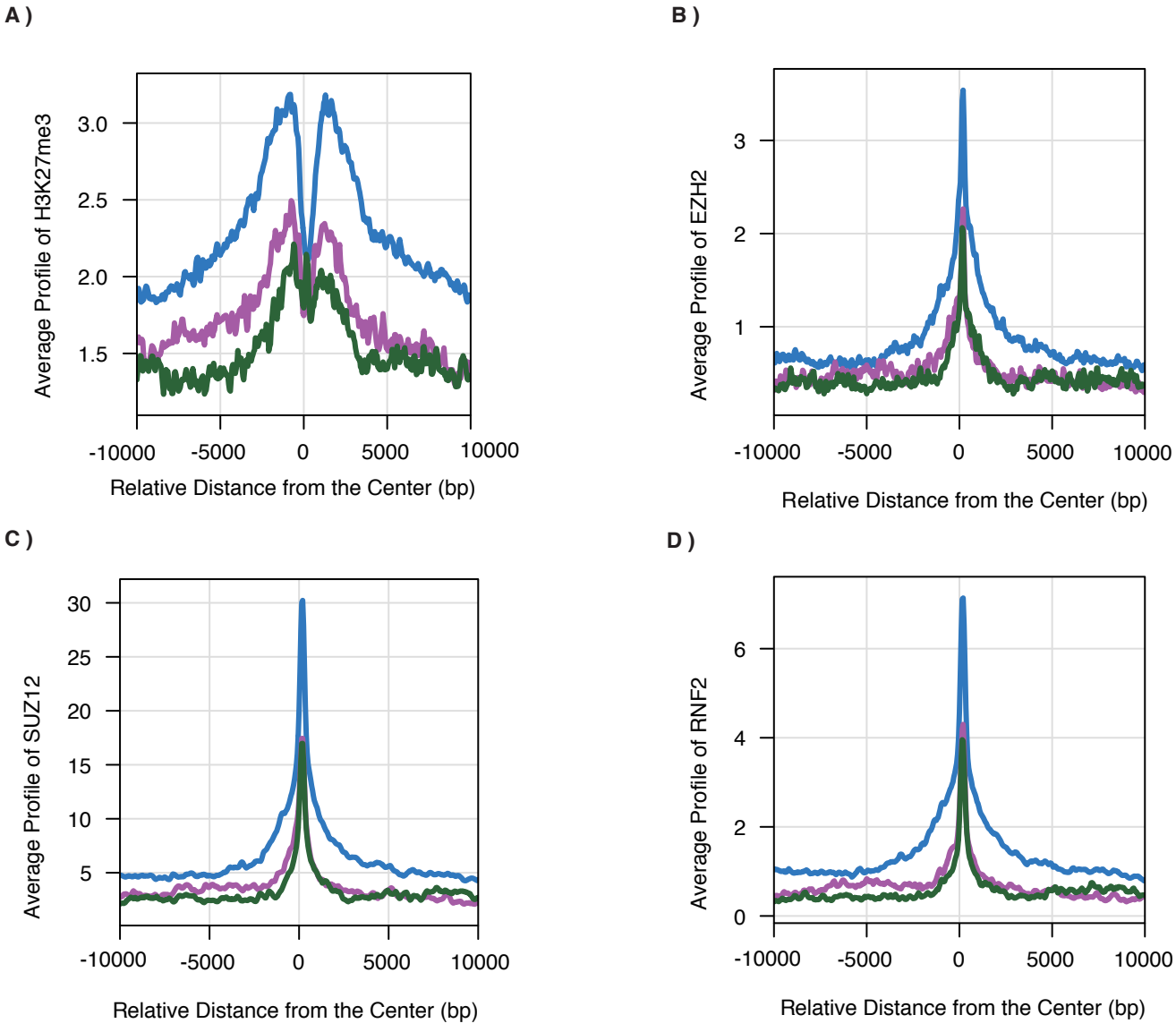
A)
Average Profile of H3K27me3
3.0
2.5
2.0
1.5
-10000
-5000
0
5000
10000
Relative Distance from the Center (bp)
B)
Average Profile of EZH2
3
2
1
-10000
-5000
0
5000
10000
Relative Distance from the Center (bp)
C)
Average Profile of SUZ12
30
25
20
15
10
5
-10000
-5000
0
5000
10000
Relative Distance from the Center (bp)
D)
Average Profile of RNF2
6
4
2
0
-10000
-5000
0
5000
10000
Relative Distance from the Center (bp)
Stringent
Moderate
Loose

Figure S10

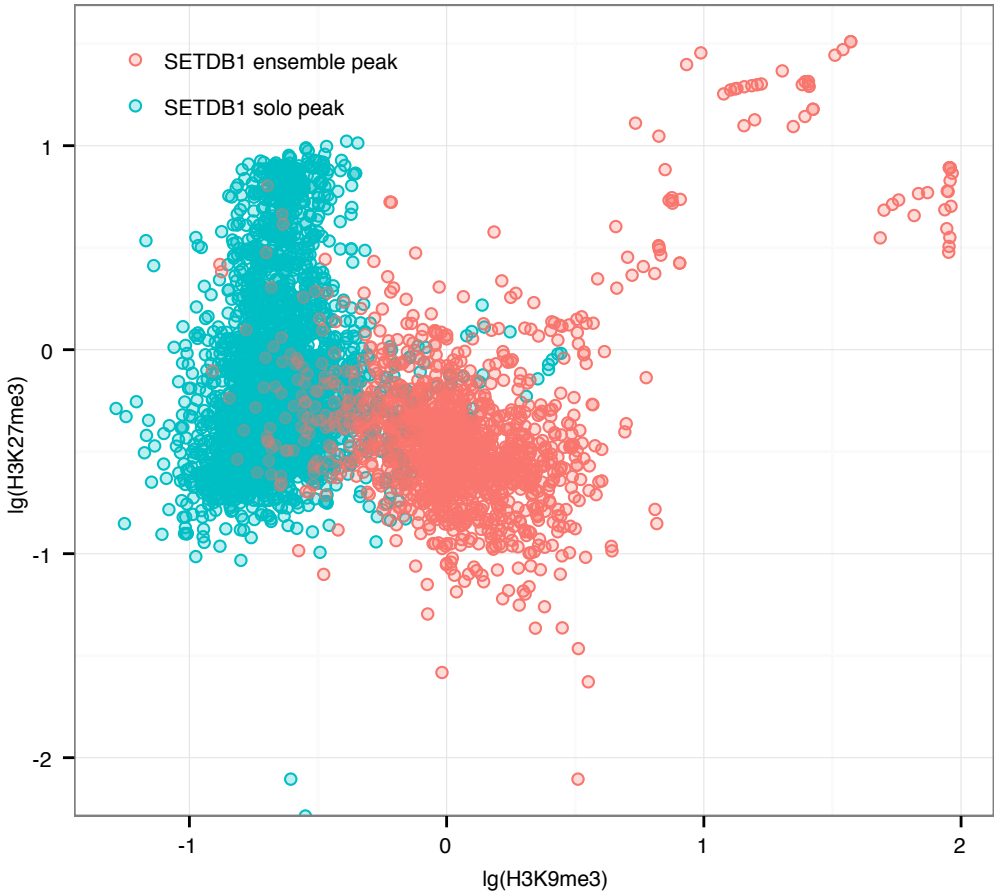
SETDB1 ensemble peak
SETDB1 solo peak
1
0
-1
-2
lg(H3K27me3)
-1
0
1
2
lg(H3K9me3)

Figure S11

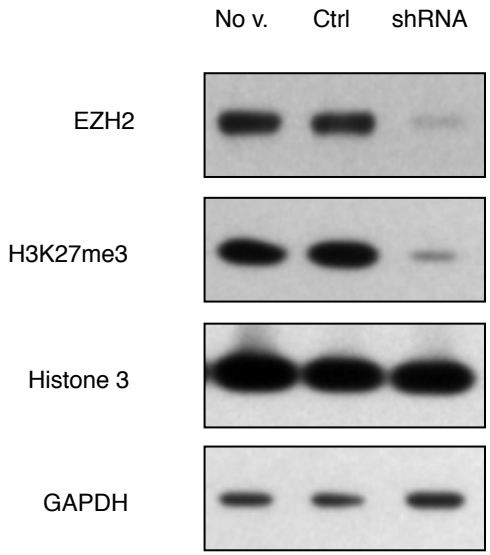

Figure S12

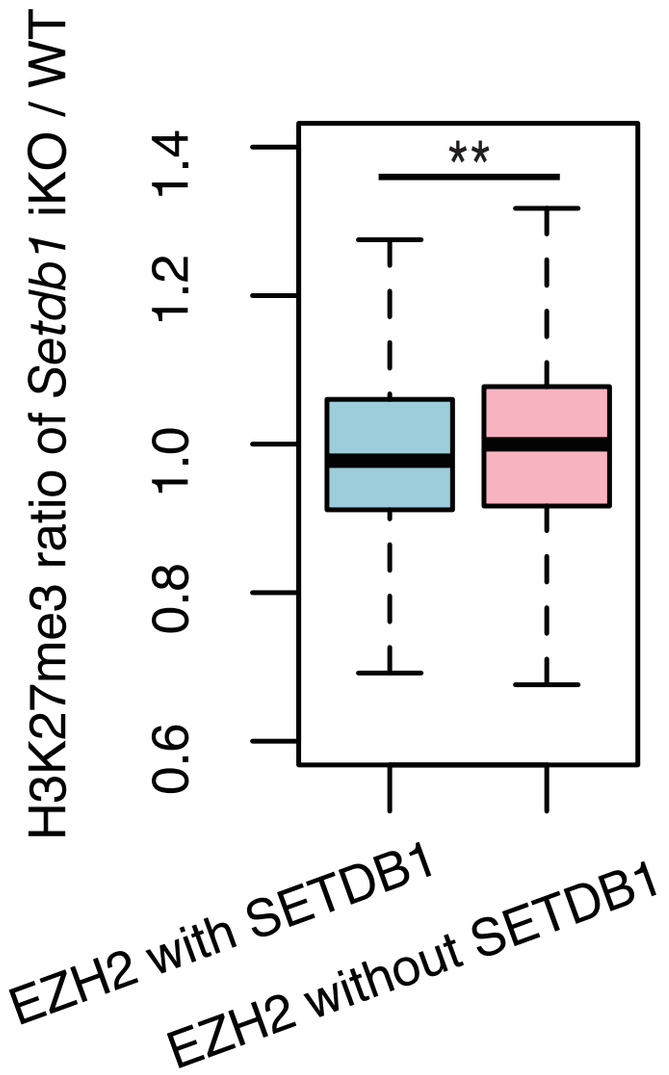
H3K27me3 ratio of Setdb1 iKO / WT
0.6
0.8
1.0
1.2
1.4
**
EZH2 with SETDB1
EZH2 without SETDB1

Figure S13

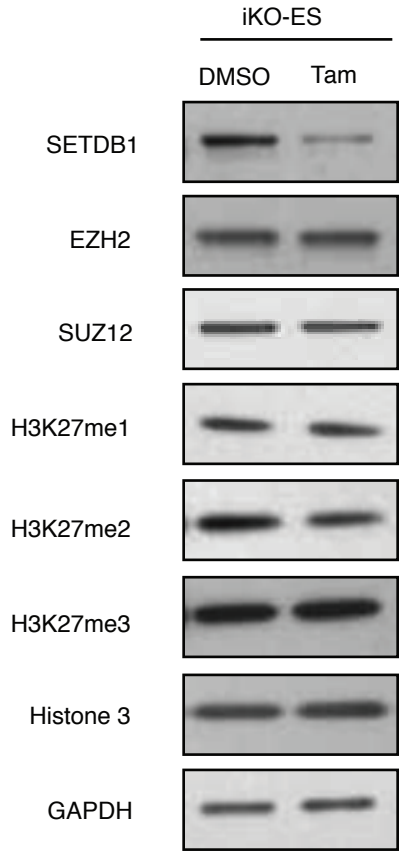
iKO-ES
DMSO
Tam
SETDB1
EZH2
SUZ12
H3K27me1
H3K27me2
H3K27me3
Histone 3
GAPDH

Figure S14

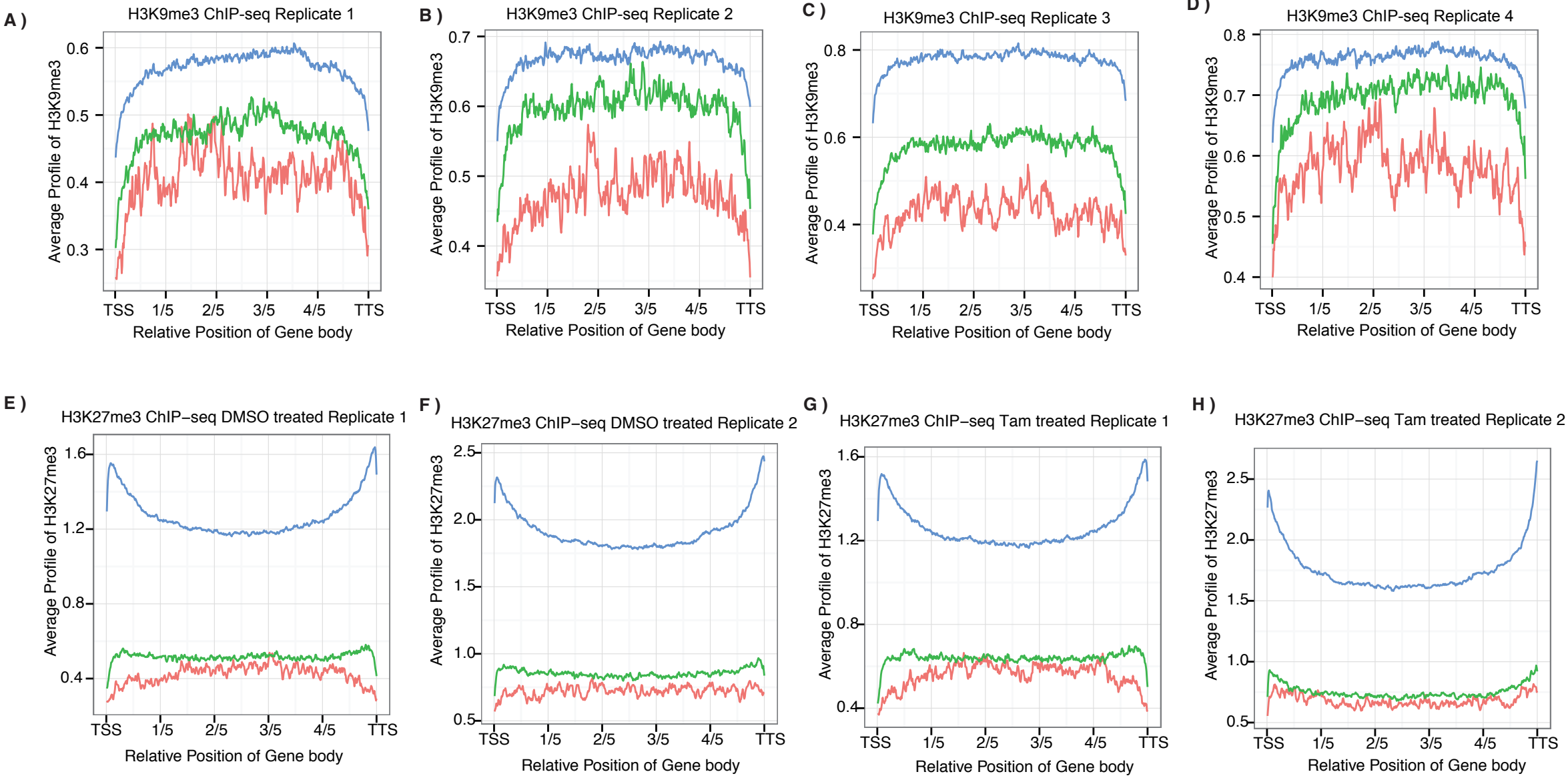
A)
H3K9me3 ChIP-seq Replicate 1
B)
H3K9me3 ChIP-seq Replicate 2
C)
H3K9me3 ChIP-seq Replicate 3
D)
H3K9me3 ChIP-seq Replicate 4
Average Profile of H3K9me3
TSS 1/5 2/5 3/5 4/5 TTS
Relative Position of Gene body
E)
H3K27me3 ChIP−seq DMSO treated Replicate 1
F)
H3K27me3 ChIP−seq DMSO treated Replicate 2
G)
H3K27me3 ChIP−seq Tam treated Replicate 1
H)
H3K27me3 ChIP−seq Tam treated Replicate 2
Average Profile of H3K27me3
I)
peak fold enrichment of H3K9me3 ChIP-seq
fold enrichment scores
replicate1
replicate2
replicate3
replicate4
J)
peak fold enrichment of H3K27me3 ChIP-seq
DMSO-treated replicate1
DMSO-treated replicate2
Tam-treated replicate1
Tam-treated replicate2
0-10
10-100
>100

Figure S15

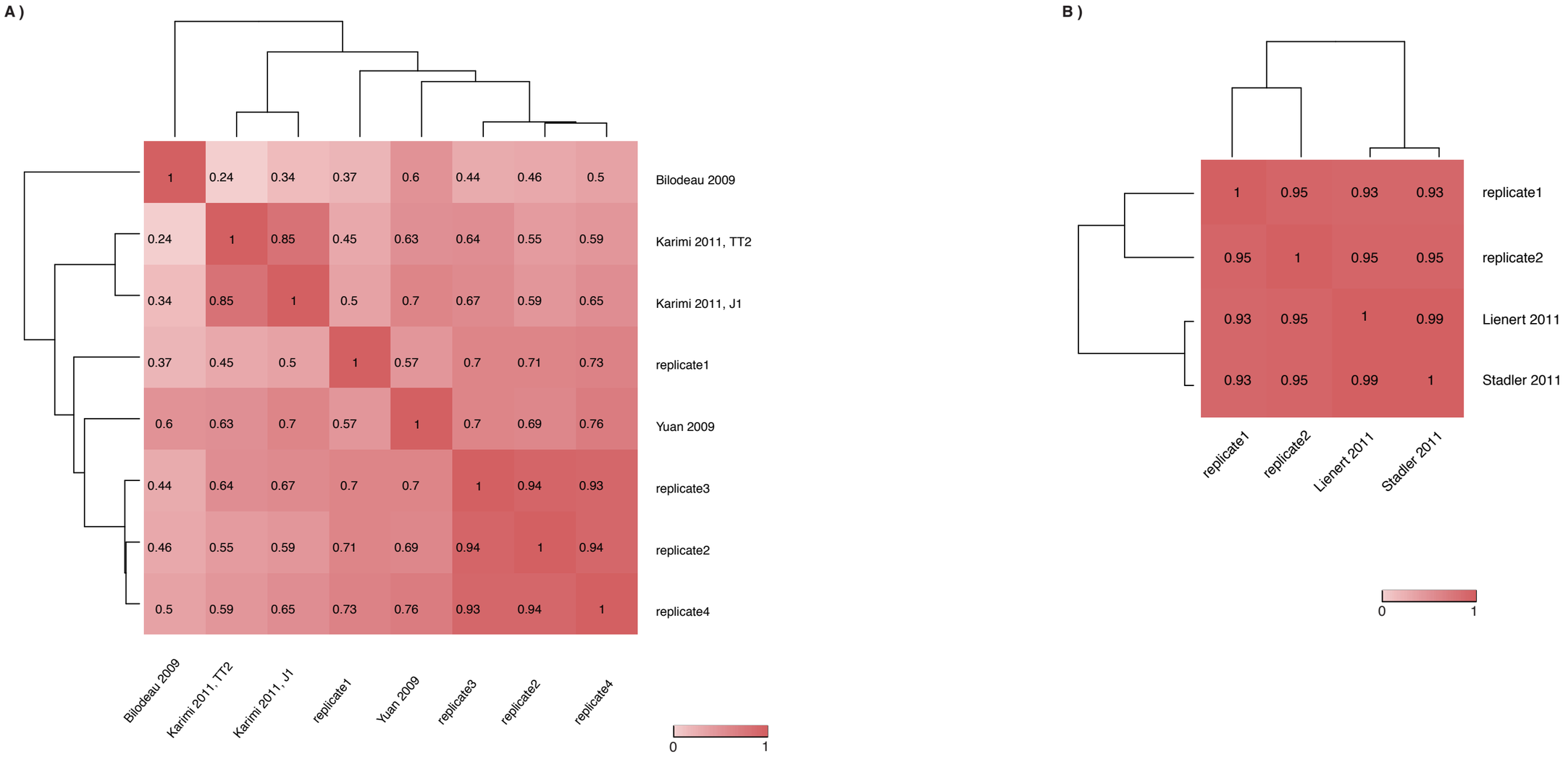
A)
1 0.24 0.34 0.37 0.6 0.44 0.46 0.5 Bilodeau 2009
0.24 1 0.85 0.45 0.63 0.64 0.55 0.59 Karimi 2011, TT2
0.34 0.85 1 0.5 0.7 0.67 0.59 0.65 Karimi 2011, J1
0.37 0.45 0.5 1 0.57 0.7 0.71 0.73 replicate1
0.6 0.63 0.7 0.57 1 0.7 0.69 0.76 Yuan 2009
0.44 0.64 0.67 0.7 0.7 1 0.94 0.93 replicate3
0.46 0.55 0.59 0.71 0.69 0.94 1 0.94 replicate2
0.5 0.59 0.65 0.73 0.76 0.93 0.94 1 replicate4
Bilodeau 2009
Karimi 2011, TT2
Karimi 2011, J1
replicate1
Yuan 2009
replicate3
replicate2
replicate4
0
1
B)
1 0.95 0.93 0.93 replicate1
0.95 1 0.95 0.95 replicate2
0.93 0.95 1 0.99 Lienert 2011
0.93 0.95 0.99 1 Stadler 2011
replicate1
replicate2
Lienert 2011
Stadler 2011
0
1